GEOPHYSICS, VOL. 79, NO. 6 (NOVEMBER-DECEMBER 2014); P. J81–J90, 9 FIGS.
10.1190/GEO2014-0134.1

Using an equivalent source with positivity for low-latitude reduction to the pole without striation

Yaoguo Li[1], Misac Nabighian[1], and Douglas W. Oldenburg[2]

ABSTRACT

We present a reformulation of reduction to the pole (RTP) of magnetic data at low latitudes and the equator using equivalent sources. The proposed method addresses both the theoretical difficulty of low-latitude instability and the practical issue of computational cost. We prove that a positive equivalent source exists when the magnetic data are produced by normal induced magnetization, and we show that the positivity is sufficient to overcome the low-latitude instability in the space domain. We further apply a regularization term directly to the recovered RTP field to improve the solution. The use of equivalent source also naturally enables the processing of data acquired on uneven surface. The result is a practical algorithm that is effective at the equatorial region and can process large-scale data sets with uneven observation heights.

INTRODUCTION

The reduction-to-the-pole (RTP) operation uses the observed magnetic data to compute the vertical magnetic field that would be observed if the magnetization were vertical. This transformation was first introduced by Baranov (1957) to deal with the asymmetry in the magnetic anomalies that is due to the oblique direction of the anomaly projection in the measurement and the nonvertical direction of the magnetization in the source bodies. The goal is to relocate the magnetic anomaly peaks directly over causative bodies. This method has been used ubiquitously in the large-scale qualitative interpretation of magnetic data. It has also gained new importance in estimating the direction of total magnetization when remanent magnetization is present (e.g., Fedi et al., 1994; Phillips, 2005; Dannemiller and Li, 2006; Gerovska et al., 2009).

Despite the plethora of methods available, RTP at low magnetic latitudes and the equator remains a major challenge. The most efficient approach to RTP is to apply the wavenumber-domain RTP operator to the Fourier transform of the observed data. However, the wavenumber-domain operation suffers from two drawbacks. First, it is unstable at low latitudes because of the noise amplification. This has prompted numerous authors to publish various methods to overcome the instability (e.g., Pearson and Skinner, 1982; Hansen and Pawlowski, 1989; Mendonca and Silva, 1993; Keating and Zerbo, 1996; Li and Oldenburg, 2001). Second, the wavenumber-domain method is only applicable when the data are located on a planar observational surface. The direct application of the wavenumber-domain method to data with highly variable observation heights, such as those from a drape survey, leads to severe phase distortion and erroneous amplitudes.

The equivalent-source technique offers an alternative means of RTP, especially under difficult conditions such as undulating observation surfaces, as first proposed by Silva (1986). In this method, an equivalent-source layer consisting of a set of dipoles in the direction of magnetization is first constructed from the observed data. The construction process is accomplished by inverting for the smallest model (Parker, 1994) that reproduces the total-field anomaly. The RTP field is then obtained by calculating the vertical magnetic field from the dipoles after they have been rotated to the vertical direction.

This approach has the advantage that it works with irregularly located data points and undulating observation surfaces. However, it still faces two major challenges: First, the equivalent-source technique ultimately suffers the same instability as the wavenumber-domain RTP operator at low latitudes. Despite the regularization, the typical striation in the declination direction associated with noise magnification still manifests itself at low magnetic latitudes. Second, as Pawlowski (1994) adeptly points out, the computational

Manuscript received by the Editor 19 March 2014; revised manuscript received 12 June 2014; published online 14 October 2014.
[1]Colorado School of Mines, Center for Gravity, Electrical, and Magnetic Studies, Department of Geophysics, Golden, Colorado, USA. E-mail: ygli@mines.edu; mnabighi@mines.edu.
[2]University of British Columbia, Department of Earth, Ocean, and Atmospheric Sciences, UBC-Geophysical Inversion Facility, Vancouver, British Columbia, Canada. E-mail: doug@eos.ubc.ca.

cost of the process can be prohibitively high, which could limit the applicability of the method.

To overcome these difficulties, we have developed a new equivalent-source RTP algorithm that incorporates a regularization function on the resultant RTP field as well as additional constraints on the underlying equivalent sources. Furthermore, the wavelet-based acceleration for equivalent-source construction makes this method feasible for large data sets.

In this paper, we assume the commonly treated scenario of a total-field anomaly produced by purely induced magnetization. We first demonstrate the challenges faced by the RTP operation at low latitudes and the equator in the spatial domain using the equivalent-source approach; these are closely related to the difficulties in the wavenumber domain. We then formulate the RTP using the equivalent source as a constrained, regularized inverse problem. We demonstrate that imposition of smoothness characteristics and bound constraints on the equivalent source can noticeably improve the quality of the recovered RTP field. We validate our procedure by using two synthetic examples and a field example.

LOW-LATITUDE REDUCTION TO THE POLE USING AN EQUIVALENT SOURCE

The equivalent-source approach to RTP was first proposed by Silva (1986) to deal with the difficulties that are well known in the wavenumber domain when working at low magnetic latitudes. The strength of the method is that the use of an equivalent source introduces regularization into the RTP process so that it is stabilized. The added benefit is that the data noise can be treated explicitly. However, moving the problem to the spatial domain does not alleviate the theoretical difficulty because the RTP operator is inherently singular at the equator in both space and wavenumber domains. As a result, although a simple regularized equivalent-source layer can stabilize the solution, it can still produce the typical artifact of striations in the declination direction. We demonstrate this aspect here.

Many different equivalent sources have been used in the literature. In the classical approach by Dampney (1969), the equivalent source is a set of point masses that reproduces the observed gravity anomaly based on the relationship between the vertical gravity anomaly and the point mass. This approach uses the same physical relationship between the observed data and their actual source in the equivalent-source construction. Recognizing that the equivalent-source construction is essentially an indirect solution of the boundary value problem associated with the Laplace's equation; however, many authors have expanded the definition of equivalent source from that of Dampney (1969) to a monopole or dipole source that reproduces the observed gravity or magnetic data simply as a potential. The corresponding relationship between observed data and the equivalent source is defined by the potential of a monopole or dipole source, and that relationship is not related to the actual physics of the data being processed. For example, Hansen and Miyazaki (1984) and Blakely (1996) use a dipole layer as the equivalent source and treat the observed magnetic data as if they were the potential produced by a dipole layer.

Let us now present a restatement of the direct formulation of RTP by equivalent sources. For the problem of RTP, it is more straightforward and superior to use the classical approach by Dampney (1969) and base the relationship between the observed magnetic data and the equivalent source on the physics of the magnetic problem because we must subsequently rotate the equivalent-source direction and then compute the corresponding vertical anomaly to obtain the desired RTP. Silva (1986) uses a set of doublets (i.e., magnetic dipole moments) aligned with the inducing field. The observed data are reproduced by the magnetic field of the dipole moment in the equivalent-source layer. Li and Oldenburg (2010) use a similar approach by parameterizing the equivalent source with the susceptibilities. The equivalent susceptibilities then lead to an equivalent magnetization under the same inducing field. The observed magnetic data are reproduced by the equivalent magnetization. In both of the approaches, the RTP is achieved by rotating the equivalent dipoles or magnetization to the vertical and then computing the corresponding vertical magnetic data. This is valid because we work with the assumption of purely induced magnetization, which is aligned with the inducing field direction. We choose to use the equivalent susceptibility for our RTP algorithm.

Assume we have a set of observed total-field magnetic anomalies $\mathbf{d} = (d_1, \ldots, d_i, \ldots, d_N)^T$. We seek to transform the magnetic-anomaly data to the RTP data $\mathbf{p} = (p_1, \ldots, p_i, \ldots, p_N)^T$ by using an equivalent susceptibility layer. The equivalent layer consists of M rectangular prisms with susceptibility values, $\mathbf{m} = (\kappa_1, \ldots, \kappa_i, \ldots, \kappa_M)^T$. The number of elements in the equivalent source is equal to, or greater than, the number of data. The observed and RTP data can be on a grid or located at scattered points on the observation surface. They are traditionally colocated but this is not necessary. The equivalent-source layer, on the other hand, is typically discretized using a uniform mesh or a semistructured mesh. When working with gridded data, it is logical to use a uniform discretization so that there is an equivalent-source element directly below each data point (Li and Oldenburg, 2010). In general, decoupling equivalent-source discretization from the data locations allows for maximum flexibility (Cordell, 1992).

The observed data $\mathbf{d}$ and RTP data $\mathbf{p}$ are related to the equivalent-source by their respective sensitivity matrices:

$$\mathbf{d} = \mathbf{G}_d\mathbf{m} \tag{1a}$$

$$\mathbf{p} = \mathbf{G}_p\mathbf{m}, \tag{1b}$$

where $\mathbf{G}_d$ and $\mathbf{G}_p$ are, respectively, the sensitivity matrices of $\mathbf{d}$ and $\mathbf{p}$ with respect to the model $\mathbf{m}$. Both are calculated easily once the magnetization direction and anomaly projection direction are specified. For $\mathbf{G}_p$, both of the directions are vertical $\hat{z}$ and for $\mathbf{G}_d$, the directions are the inducing field direction $\hat{\mathbf{B}}_0$ (assuming that $\mathbf{d}$ represent a total-field anomaly). The elements of the matrices are the respective magnetic anomaly produced at the ith location by a unit susceptibility in the jth cell of the discretized equivalent source,

$$g_{dij}(\mathbf{r}_i) = \frac{B_0}{4\pi}\int_{\Delta V_j}\frac{\partial^2}{\partial \hat{B}_0^2}\frac{1}{|\mathbf{r}' - \mathbf{r}_i|}\,dv', \tag{2a}$$

$$g_{pij}(\mathbf{r}_i) = \frac{B_0}{4\pi}\int_{\Delta V_j}\frac{\partial^2}{\partial z^2}\frac{1}{|\mathbf{r}' - \mathbf{r}_i|}\,dv', \tag{2b}$$

where $\partial/\partial\hat{B}_0$ denotes the derivative in the direction $\hat{B}_0$. The second-order vertical derivative in equation 2b corresponds to the rotation of magnetization and magnetic-anomaly projection to the vertical. (We adopt a Cartesian coordinate system with x-axis pointing north and z-axis pointing vertically downward.)

As indicated above, the RTP operation via an equivalent-susceptibility layer is a two-step process. First, we construct an equivalent-susceptibility layer $\mathbf{m}$ that satisfies equation 1a. We then compute the RTP field according to equation 1b. In the direct formulation, the source construction step is carried out independently from the RTP calculation. Therefore, the inverse problem is concerned only with the equivalent-source construction, and the characteristics of the RTP field are disregarded.

To stabilize the equivalent-source solution and deal with the noise in the data, a regularized solution is obtained by minimizing a weighted sum of the data misfit and model objective function of the source:

$$\phi = \|\mathbf{W}_d(\mathbf{d}^{\text{obs}} - \mathbf{G}_d\mathbf{m})\|_2^2 + \beta\|\mathbf{W}_m\mathbf{m}\|_2^2, \qquad (3)$$

where the first term is the data misfit function and the second term is the model objective function quantifying the complexity of the equivalent source, and the scalar β is a regularization parameter chosen such that the data misfit is consistent with the noise level in the data. In equation 3, $\mathbf{d}^{\text{obs}}$ is the observed total-field magnetic anomaly, $\mathbf{W}_d$ is a diagonal data-weighting matrix consisting of the inverse of the noise standard deviation, and $\mathbf{W}_m$ is a model weighting matrix defining the structural complexity of the model to be recovered. Different choices are possible. For instance, Silva (1986) uses an identity matrix that leads to a smallest model formulation; we use a discretized form of the objective function consisting of a weighted sum of the smallest and flattest model (norm of the gradient) components. The solution of this inverse problem yields the desired equivalent source and, therefore, the RTP field that we seek to construct.

As an illustration, we now apply this approach to a simple synthetic model that has been used by previous authors for testing RTP algorithms (e.g., Hansen and Pawlowski, 1989) and reduce to the pole the total-field anomaly calculated at the magnetic equator. The target consists of a single prism in a nonsusceptible background. The prism has a width of 20 units in both horizontal directions, a thickness of two units, a depth to the top of one unit measured from the observation plane, and magnetization of 0.35 A/m. The total-field anomaly is calculated over a 64-by-64 grid with an interval of one unit in each direction. The total-field magnetic anomaly produced by the prismatic source with an induced magnetization at the pole and the equator are shown in Figure 1. All data are on a planar surface. To simulate noisy observations, we have contaminated the data at the equator by Gaussian random noise with a 1-nT standard deviation.

We have applied the above-described direct formulation to reduce the data to the pole by using cell-based susceptibilities as the equivalent source and a smallest model objective function, and fitting the noisy data in Figure 1b to the expected data misfit. The resulting RTP data and the equivalent susceptibility are shown in Figure 2. We note that the RTP field is stable even at the equator because of the regularization used in the equivalent-source construction, which has been demonstrated by Silva (1986). Compared with the true RTP data in Figure 1a, however, the recovered RTP data exhibit several noticeable artifacts. Two negative side lobes to the west and east of the main positive peak are lost, and there are zones of noisy background aligned in the declination direction of the original data.

Although the regularization has stabilized the RTP solution, the fundamental difficulties of reconstructing the RTP field from observations at low-magnetic latitudes are still severely affecting the quality of the recovered RTP data. The cause of the artifacts is the elongated negative zones in the equivalent susceptibility (Figure 3). These negative zones occur because it is easiest to reproduce the negative values in the data (Figure 1b) with the negative susceptibilities.

We propose an improved formulation to overcome these difficulties. The new formulation first imposes a regularization directly on the recovered RTP data so that its noisy background can be sup-

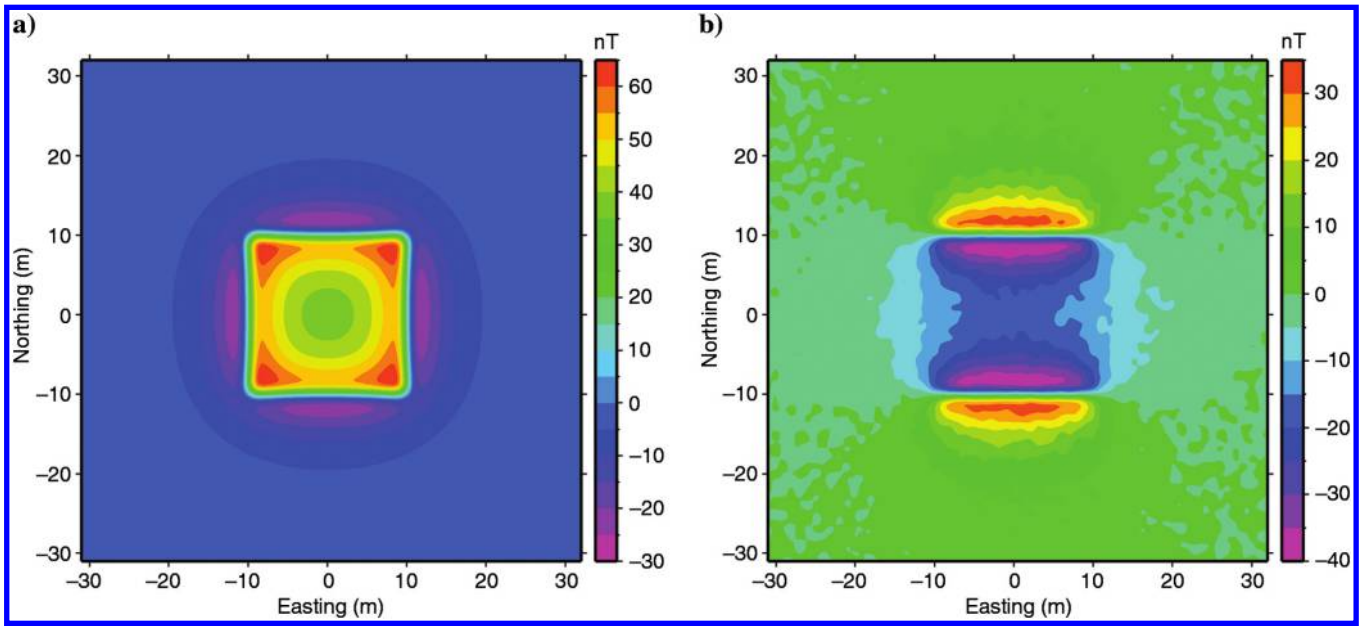

Figure 1. (a) Total-field magnetic anomaly at the pole. (b) Total-field anomaly at the equator with a declination $D = 0°$. The anomaly at the equator has been contaminated by Gaussian noise to simulated noisy observations. The causative body is a rectangular prism with a width of 20 units in both horizontal directions, a thickness of two units, a depth to the top of one unit, and magnetization of 0.35 A/m aligned with the inducing-field direction.

pressed. Second, and more importantly, we impose a positivity constraint on the equivalent source to prevent the occurrence of negative susceptibility and, thereby, reduce the striation typically associated with the low-latitude RTP. We address these in the next section.

AN ALTERNATIVE FORMULATION

Regularizing reduction-to-the-pole field

We propose an alternative approach in which the RTP field is treated explicitly as the model in the inverse procedure and regularize the RTP solution by directly minimizing an objective function of it subject to the data constraint. Let $\mathbf{p}$ be the vector representing the RTP field. We define the model objective function as

$$\phi_p = \|\mathbf{W}_p\mathbf{p}\|_2^2, \tag{4}$$

where $\mathbf{W}_p$ is a model weighting matrix, which can be any form commonly used to measure the roughness or structural complexity of a model. We choose a $\mathbf{W}_p$ derived by discretizing the weighted combination of the smallest model and flattest model (Parker, 1994) using a finite-difference approximation of the derivatives over a regular grid:

$$\phi_m = \int\int (\alpha_s p^2 + |\nabla p|^2)\mathrm{d}x\mathrm{d}y, \tag{5}$$

where p is the function representing the RTP field and $\alpha_s << 1$ and determines the trade-off between the smallest and flattest components. Substituting equation 1b into equation 4 yields

$$\phi_p = \|\mathbf{W}_p\mathbf{G}_p\mathbf{m}\|_2^2. \tag{6}$$

This model objective function is expressed in the equivalent source but ultimately measures the structural complexity of the RTP field to be recovered.

Using the same data misfit function as in the direct formulation in equation 3, our new inverse formulation is defined by the following optimization problem:

$$\phi = \|\mathbf{W}_d(\mathbf{d}^{\mathrm{obs}} - \mathbf{G}_d\mathbf{m})\|_2^2 + \beta\|\mathbf{W}_p\mathbf{G}_p\mathbf{m}\|_2^2. \tag{7}$$

Minimization of this objective function with a suitably chosen value of β yields an equivalent source that minimizes the structural complexity of the final RTP field and reproduces the total-field data. This objective function is similar to that in equation 3 in appearance, but has a different meaning. In this formulation, we treat the RTP data $\mathbf{p}$ as the model, and the forward mapping from $\mathbf{p}$ to $\mathbf{d}$ is defined as a parametric functional by equations 1. It is well understood that applying the regularization to the model of the inverse problem is preferred in general. Although the inverse problem is expressed in the equivalent source $\mathbf{m}$, it only serves as an auxiliary variable relating the RTP field $\mathbf{p}$ to the total-field anomaly $\mathbf{d}$. We are not concerned about the specific behavior of $\mathbf{m}$ so long as it reproduces the data and yields a good RTP field.

Differentiating ϕ in equation 7 with respect to $\mathbf{m}$ and setting the gradient to zero yields the normal equation to be solved for the equivalent source:

$$(\mathbf{G}_d^T\mathbf{W}_d^T\mathbf{W}_d\mathbf{G}_d + \beta\mathbf{G}_p^T\mathbf{W}_p^T\mathbf{W}_p\mathbf{G}_p)\mathbf{m} = \mathbf{G}_d\mathbf{W}_d\mathbf{d}^{\mathrm{obs}}. \tag{8}$$

Inverting this system of linear equations yields the equivalent source that produces the RTP field with the minimum structure as measured by equation 4.

The matrix system in equation 8 involves two dense matrices, $\mathbf{G}_d$ and $\mathbf{G}_p$. For large data sets, the memory requirement and CPU time can become prohibitively high. Fast numerical algorithms are required to obtain the solution with efficiency for practical use. We have adopted the conjugate gradient (CG) solver by using fast algorithms for matrix-vector products. In this approach, we construct a

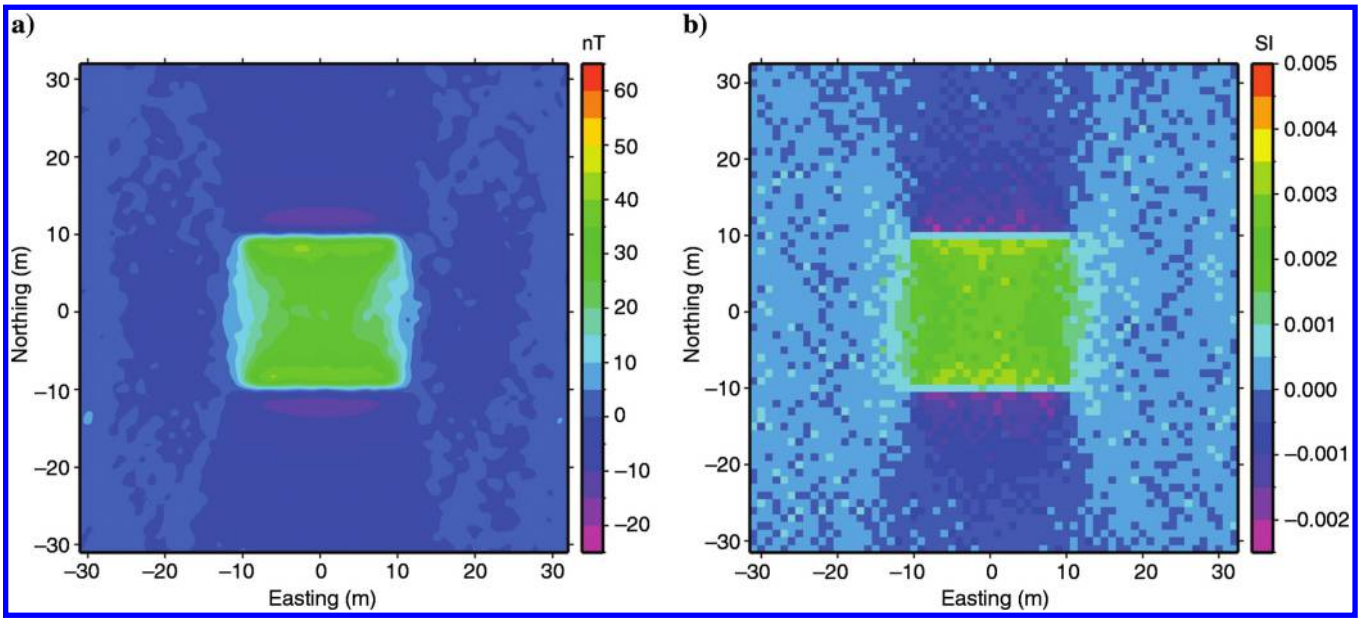

Figure 2. Result of the RTP by equivalent source. (a) RTP data calculated from a smallest model that is constructed from the noisy data in Figure 1b. (b) The equivalent susceptibility. With the regularization determined by the noise level in the data, the RTP solution is stable. Compared with the true field in Figure 1b, however, the RTP solution exhibits several noticeable artifacts.

sparse representation of each sensitivity matrix using discrete wavelet transforms based on compactly supported orthonormal wavelets (Daubechies, 1992). For gridded data, the algorithm designed for rapid equivalent-source construction by Li and Oldenburg (2010) is used. For general data sets with observations located along flight lines, the equivalent source construction by Davis and Li (2011) can be used. In both methods, the major computational effort is in the generation of the two sensitivity matrices when applying the wavelet compressions, and this component incurs the most computational cost of using an equivalent-source method to perform RTP. It is also important to note that the matrix $\mathbf{A} = (\mathbf{G}_d^T \mathbf{W}_d^T \mathbf{W}_d \mathbf{G}_d + \beta \mathbf{G}_p^T \mathbf{W}_p^T \mathbf{W}_p \mathbf{G}_p)$ in equation 8 is never formed explicitly when using a CG solver because we can efficiently compute the result of multiplying the matrix with a vector in CG iterations through the multiplications of individual components forming the matrix.

We remark that any fast numerical method can be used in solving equation 8 to construct the equivalent source in the above algorithm. The details of the numerical strategy only pertain to the efficiency of the solution, and they do not directly impact the characteristics of the recovered RTP data. For this reason, we choose not to specify the implementation here and hope that the flexibility will allow the use of various efficient solution strategies.

We choose an equivalent source consisting of a set of contiguous vertical cubes of one unit on a side. The equivalent source is placed at a depth to top of 0.5 unit, which is above the actual source depth in this example. This depth is chosen because we want the equivalent layer to be as close as possible to the observation surface but not directly at the observation surface. Our numerical experiments suggest that a depth comparable to the nominal grid spacing works well as a general purpose choice.

Figure 3 displays the RTP result obtained by the new approach that directly imposes a model objective function on the RTP field with the parameter $\alpha_s = 0.0001$ in equation 5. In the same way as before, an optimal regularization parameter β is chosen to achieve the expected data misfit. It clearly shows the central high above the causative body. There are, however, only two negative side lobes and also visible striation in the north–south direction. This is the most severe situation because the inducing field inclination is zero. The striation will become weaker as the inclination increases. Over all, we have a reasonably well-recovered RTP field as can be seen from the comparison with Figure 1a.

Constraining equivalent susceptibility

The above formulation effectively suppresses the noise in the recovered RTP and generates a robust solution with fewer undesirable characteristics. The algorithm achieves the desired stability at low magnetic latitudes, which has been the main concern in the wavenumber-domain approaches and thus improves upon the existing equivalent source-based RTP approach. However, the results are not free from one common artifact of many RTP algorithms; namely, the recovered RTP field still has striations and broader negative lobes in the declination direction. This is to be expected because a flattest-model solution in the spatial domain is equivalent to a spectrally weighted smallest model solution in the wavenumber domain, and such a solution will have broad striations because it still has the spectral notches in the declination direction (Li and Oldenburg, 2001). For this reason, the corresponding result will not be free of the said drawbacks unless additional constraints are imposed on the recovered spectral content of the RTP field.

In the wavenumber domain, Li and Oldenburg (2001) choose to apply a flattest model objective function to the Fourier transform of the RTP field. The requirement of a flattest RTP power spectrum provided enough prior information to prevent the occurrence of the notch in the power spectrum of RTP field aligned with the declination. This improvement significantly reduces the striation of RTP field in the space domain.

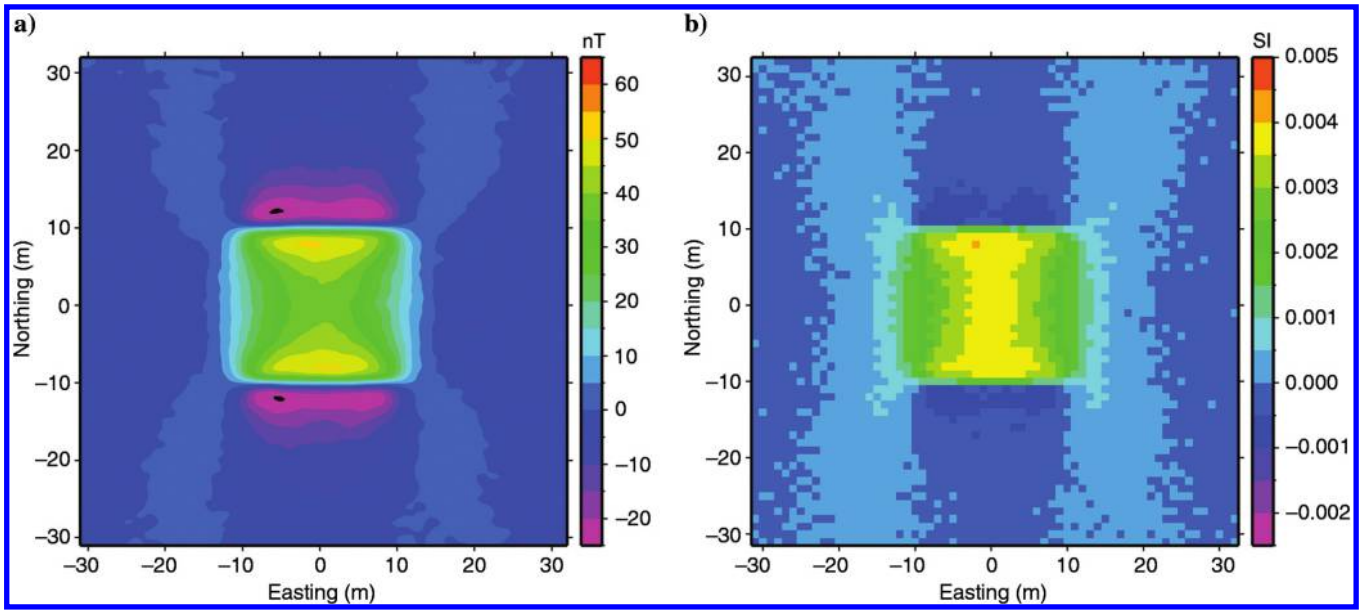

Figure 3. (a) RTP field recovered through the inversion of the noisy total-field anomaly at the equator shown in Figure 1b. (b) Corresponding equivalent susceptibility. A model objective function is applied directly to the desired RTP field. Compared with the RTP field recovered in the preceding section, this result is much less affected by noise in the background and shows four noticeable side lobes. However, elongated artifacts are still visible.

The question is then: What would be a similar constraint on the equivalent source in the space domain for our current approach? Examination of the equivalent source constructed for the case in Figure 3 shows that the equivalent susceptibility consists of a positive zone directly below the main anomaly, but there are zones of negative equivalent susceptibility north and south of the positive zone. These negative zones also extend along the declination direction. It is clear that these zones are the cause of the striation in the recovered RTP field.

Based on the above observation, we surmise that restricting the equivalent source to being entirely positive might reduce the undesirably broad negative lobes in the RTP field and the striation. Implementation of positivity requires the inclusion of a bound constraint in the minimization problem. Our numerical experiments with synthetic and field examples have shown that this simple constraint can dramatically improve the quality of the recovered RTP field. The associated optimization problem then becomes

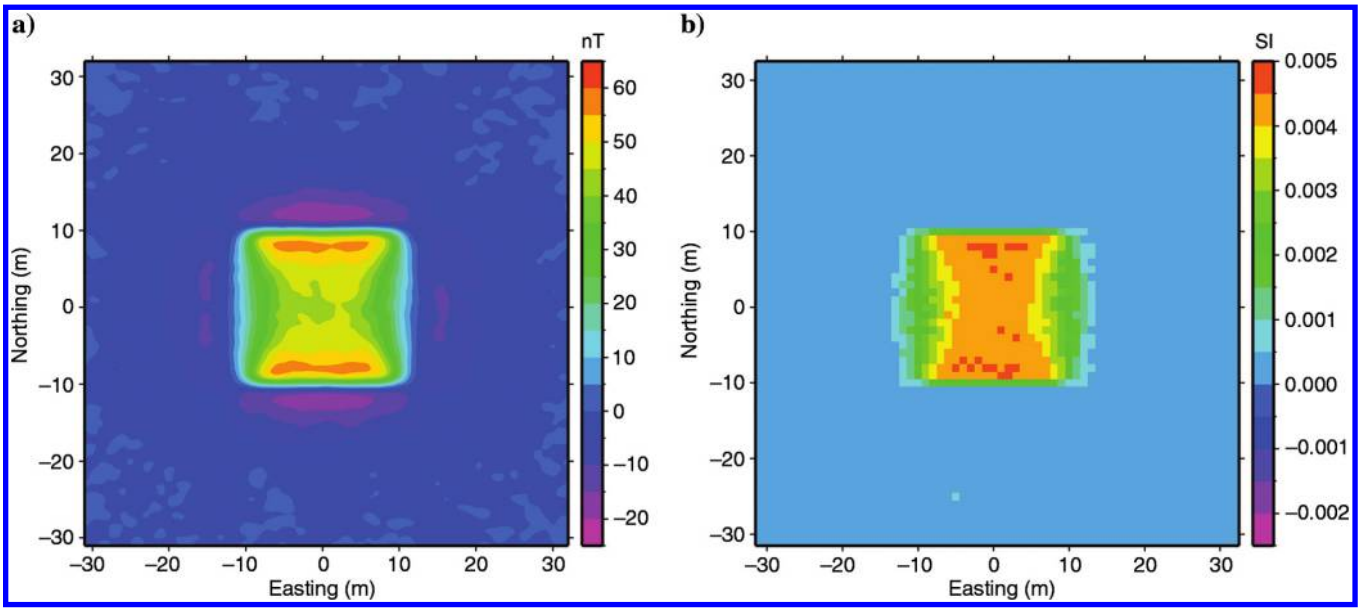

Figure 4. (a) RTP field recovered through the inversion of the noisy total-field anomaly at the equator. (b) Corresponding equivalent susceptibility. A model objective function applied directly to the desired RTP field, and a positivity constraint is applied to the equivalent source. Compared with the RTP fields recovered in the preceding sections, this result is most consistent with the true field at the pole (Figure 1).

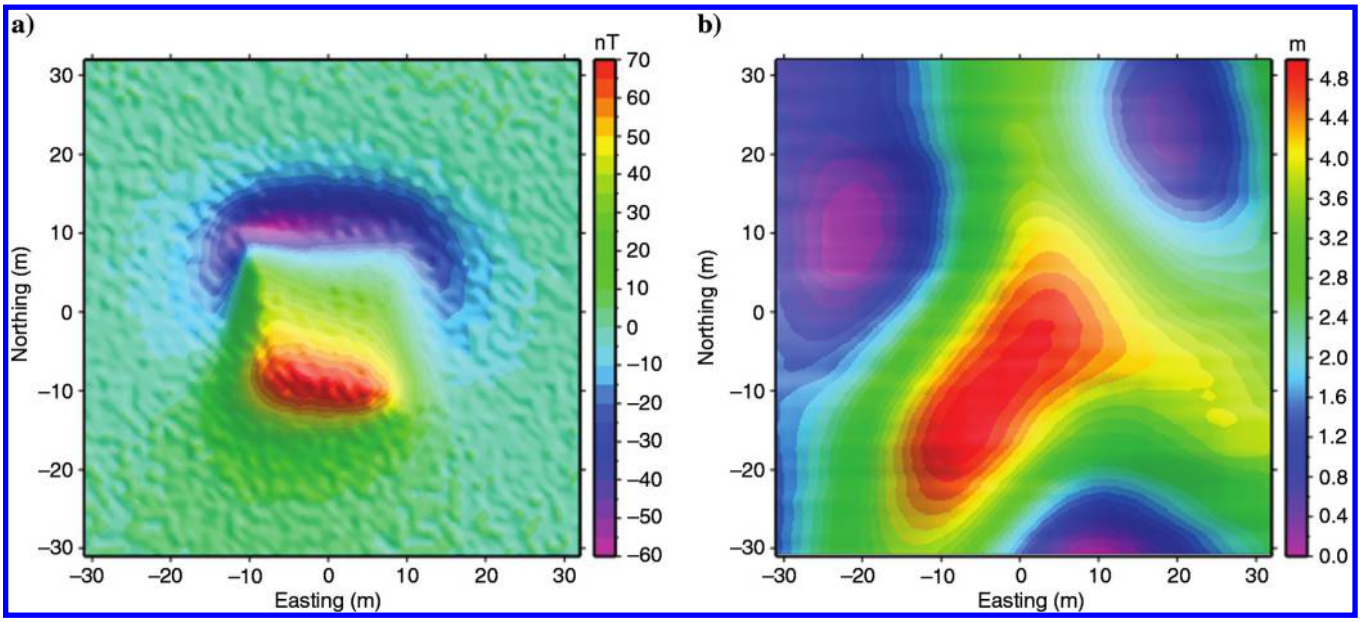

Figure 5. Synthetic example with undulating observational surface. (a) A set of simulated noisy total-field data at midlatitude, $I = 50°$, $D = 10°$. (b) Undulating observation surface. The causative body is the same as that used to generate the data in Figure 1.

$$\begin{aligned} &\text{minimize} \quad \phi = \|\mathbf{W}_d(\mathbf{d} - \mathbf{G}_d\mathbf{m})\|_2^2 + \beta\|\mathbf{W}_p\mathbf{G}_p\mathbf{m}\|_2^2 \\ &\text{subject to} \quad \mathbf{m} \geq \mathbf{0} \end{aligned}. \quad (9)$$

Many options are available for carrying out the bound-constrained minimization. We choose to use the interior-point method (IPM). It works well with our choice of CG solver for the linear system of equations. The final algorithm requires two levels of iteration: the inner iteration for the CG solver embedded in the outer iteration of the IPM. Readers are referred to Wright (1997) and Nocedal and Wright (1999) for general IPM theory, and to Li and Oldenburg (2003) for implementation details in potential-field methods.

Figure 4 displays the RTP result obtained by imposing the positivity constraint on the equivalent source while keeping everything else such as data misfit the same as before. The constructed equivalent susceptibility has an area of concentrated high values and does not show any elongated negative zones. The corresponding RTP data show the central high above the causative body and four negative side lobes of comparable magnitudes. There is no longer visible striation in the north–south direction. This is an excellent

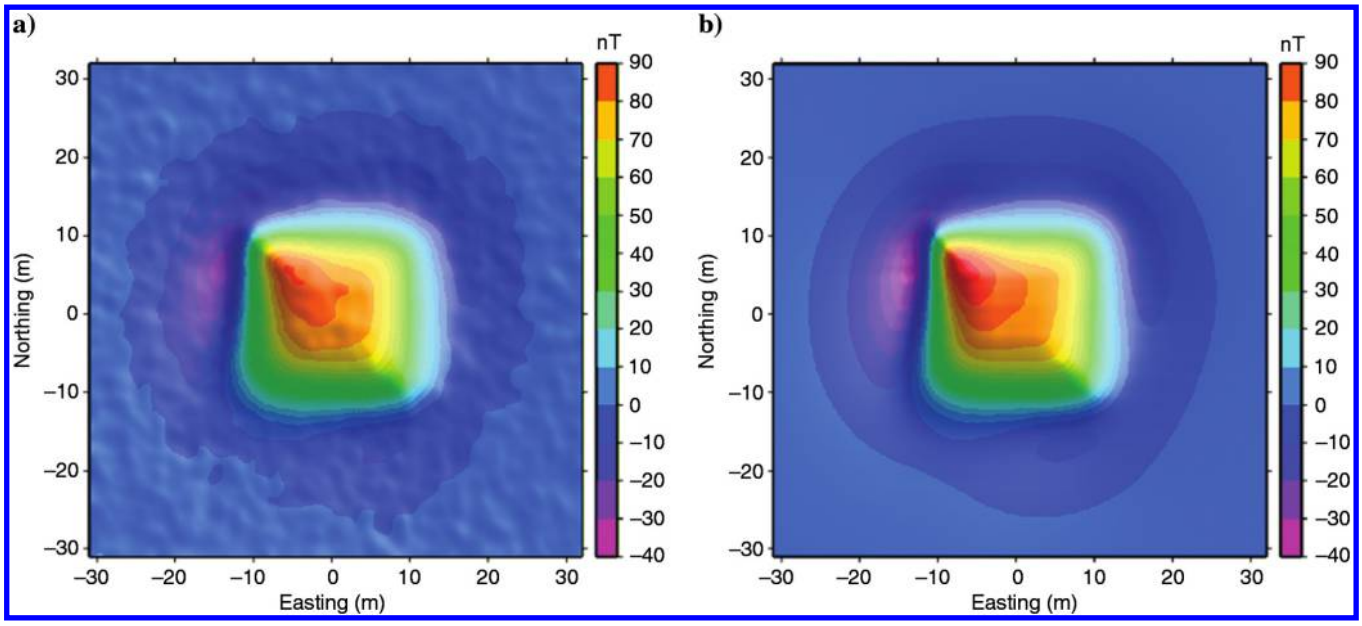

Figure 6. Recovered RTP field on the undulating surface (a) and the true field at the pole (b) on the same observation surface (Figure 5b).

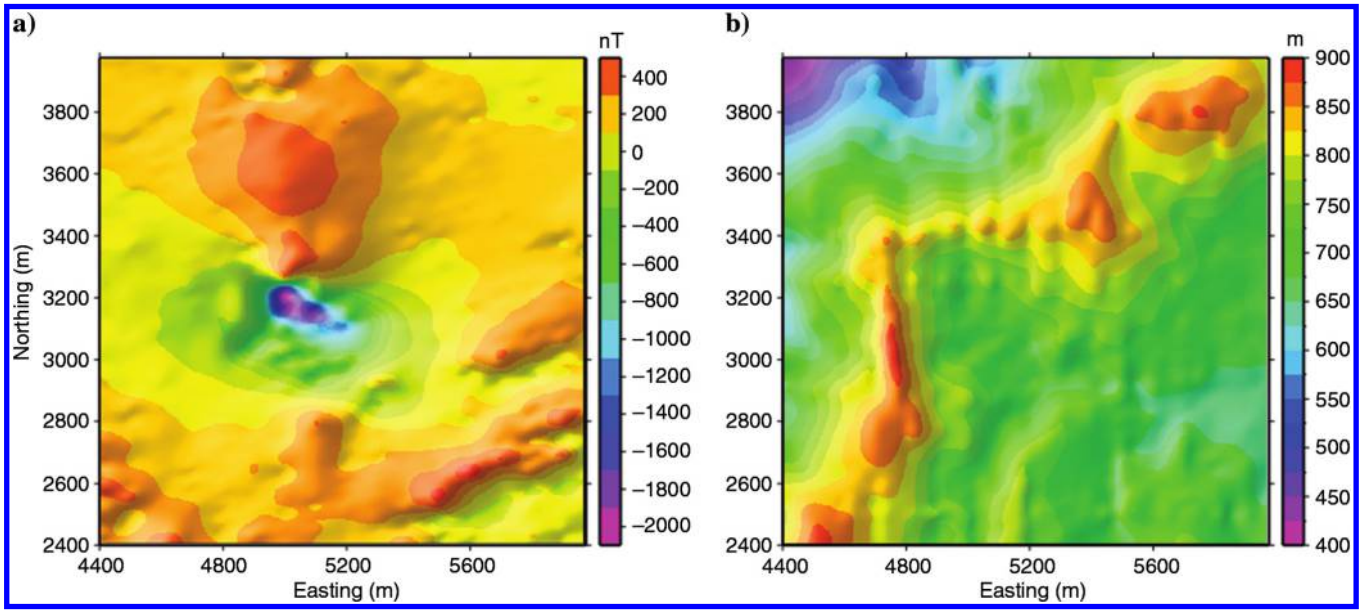

Figure 7. A field example illustrating the low-latitude RTP using equivalent sources. (a) Total-field anomaly. (b) Elevation of the observation surface. The inducing field has an inclination of −17° and declination of 1.5°.

representation of RTP data as can be seen from the comparison with Figure 1a. In fact, there is little indication of striations along the declination of the original data. Thus, the positivity constraint is shown to be a crucial condition in this case, and it has enabled the recovery of the high-fidelity RTP field.

Existence of all-positive equivalent sources

We have demonstrated that an all-positive equivalent source yields superior RTP results. We are able to construct an entirely positive equivalent source numerically that reproduces the observed data to a misfit level consistent with the contaminating noise. However, a theoretical question remains whether a positive equivalent source always exists for a set of total-field magnetic data.

Assuming that the observed magnetic anomaly is produced by a purely induced magnetization, and assuming that we use a dipole-based equivalent source whose direction is aligned with the inducing field, the answer to this question is: Yes, such a positive equivalent source does exist. A complete proof is given in the Appendix A, and we summarize the main result here.

Let us assume that the vertical magnetic field is produced by a vertical magnetic dipole. The strength of the equivalent vertical magnetization layer at a given depth h that reproduces the observed field can be shown to be proportional to the pseudogravity field of the magnetic dipole (equation A-14 in Appendix A):

$$m(x', y', h) = 2g_{\text{pseudo}}(x', y', h), \tag{10}$$

where $m(x', y', h)$ is the magnetization strength, g_{pseudo} the pseudogravity, (x', y') are the coordinates of equivalent source in the plane at depth h. The pseudogravity (Baranov, 1957) corresponding to a magnetic dipole is positive because it is produced by a positive point mass. It follows that the equivalent magnetization strength is positive. Correspondingly, the equivalent susceptibility is also positive when the inducing field is used to set up the equivalent magnetization.

The magnetic anomaly due to a general causative body is a linear superposition of dipole fields. Therefore, the conclusion from the dipole field is directly applicable to the field due to extended sources. The magnetic anomalies located away from the pole are given by the rotations of the anomaly projection and the magnetization direction. These rotations are independent of the magnetization strength. Thus, the positivity proof holds true for all cases in which the magnetization direction is the same as that of the inducing field. The positivity constraint used in our RTP formulation is a theoretical requirement.

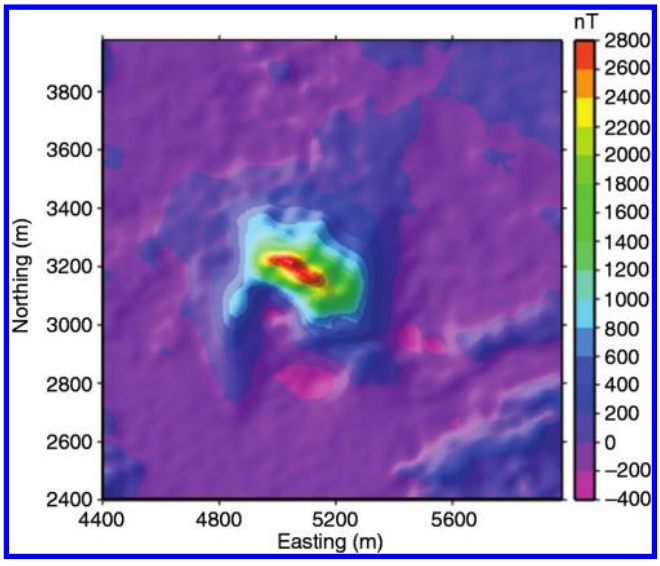

Figure 8. Recovered RTP field from the total-field anomaly shown in Figure 7a. The RTP anomaly is colocated with the original data on the topographic surface (Figure 7b).

ADDITIONAL EXAMPLES

To complete our illustration, we apply the method to a synthetic data set simulated on an undulating surface. Figure 5a displays the simulated noisy total-field anomaly on the observation surface in Figure 5b. The inducing field has an inclination of 50° and declination of 10°. The asymmetry due to the variation in the data elevation is visible. We have used a similar equivalent layer as in the previous example. Figure 6a is the recovered RTP field by taking into consideration the observation elevations and constructing a positive equivalent source. This result compares well with the true field at the pole on the same observation surface (Figure 6b). This example serves to demonstrate that the reformulated algorithm maintains the capability of the equivalent-source RTP method when working with observations on uneven surfaces, for which the wavenumber-domain method is no longer applicable.

As a final example, we apply our equivalent-source RTP method to a set of field data acquired in gold exploration at low magnetic latitude ($I = -17°$ and $D = 1.5°$). Figure 7 displays the total-field anomaly observed on a topographic surface. The elevation of the topography varies from 400 to 900 m. The influence of the rugged topography and the low-latitude projection is clearly visible in the data. The resultant RTP field is shown in Figure 8, which shows a compact anomaly over a generally nonmagnetic background.

CONCLUSION

We have reformulated the equivalent source-based method for reduction to the pole by treating the RTP field as the model and the equivalent source as an auxiliary variable that maps the RTP field to the observation. This allows one to apply a user-designed model objective function directly to the desired RTP field so that the stability at low latitude is achieved and the data noise is treated. We have demonstrated that, although a simple flatness objective function in the spatial domain can produce a good result, it does not completely eliminate the elongating features. Incorporating positivity on the equivalent source improves the result and greatly reduces the undesirable artifacts. The numerical solution is accelerated by using the fast matrix-vector multiplications based on wavelet compression, so the method is applicable to large-scale data sets. In addition, the equivalent-source method naturally lends itself to the processing of data acquired on uneven surfaces, which cannot be processed with wavenumber-domain methods. Thus, we have developed an RTP algorithm that is stable at low magnetic latitudes and the equator, suppresses striation, and is applicable to large-scale data sets acquired from drape surveys.

ACKNOWLEDGMENTS

The first author wishes to thank K. Davis and M. A. Kass for continually reminding him to write up this work and for many in-

sightful discussions. We thank H. Rim for his assistance in the preparation of the manuscript. We would like to thank P. Eaton and Newmont Mining Corporation for supplying the field data set used in this study. We thank the associate editor V. Barbosa, reviewers M. Fedi, V. C. Oliveira Jr., and F. Caratori Tontini, and an anonymous reviewer for their graciously positive and insightful comments. This work was supported in part by the Gravity and Magnetics Research Consortium (GMRC). The current sponsoring companies of GMRC are Anadarko, Bell Geospace, BG Group, BGP, BP, CGG, ConocoPhillips, ExxonMobil, Gedex, Lockheed Martin, Marathon Oil, Microg LaCoste, Shell, Petra Energia, Petrobras, Tullow Oil, and Vale.

APPENDIX A

EXISTENCE OF AN ALL-POSITIVE EQUIVALENT SOURCE LAYER

One critical condition in obtaining stable and high-fidelity RTP results using the proposed method is the positivity of the equivalent source layer. In this appendix, we prove the existence of such an equivalent source to provide the theoretical basis for imposing such a constraint.

At the pole, the equivalent layer placed above the true causative body is magnetized in a vertical direction and one measures the vertical component of the magnetic field (true RTP field). The vertical magnetic component of a vertical magnetic dipole at a depth h below the observational surface $z = 0$ (Figure A-1) is given by

$$B_{z,\text{dipole}} = \frac{\mu_0 m}{4\pi}\frac{1}{r^3}(3\cos^2\theta - 1) = \frac{\mu_0 m}{4\pi r^3}\left(3\frac{h^2}{r^2} - 1\right), \tag{A-1}$$

where m is the magnetic moment of the dipole and $r = \sqrt{(x-\xi)^2 + (y-\eta)^2 + h^2}$. The observed vertical magnetic field at the point $(x, y, 0)$ is obtained by integrating equation A-1 over the equivalent layer surface:

$$B_z = \frac{\mu_0}{4\pi}\int_{-\infty}^{\infty}\int_{-\infty}^{\infty} m(\xi,\eta,h)\left(\frac{3h^2}{r^5} - \frac{1}{r^3}\right)\mathrm{d}\xi\mathrm{d}\eta. \tag{A-2}$$

Because A-2 is a convolution integral, we write it as

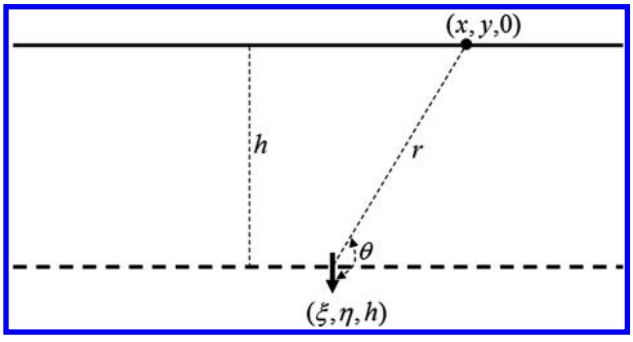

Figure A-1. Definition of the quantities used in the proof of the positivity of equivalent source. The dipole is located at (ξ, η, h), and the data are observed on the plane $z = 0$.

$$\mathcal{F}(B_z) = \frac{\mu_0}{4\pi}\mathcal{F}(m)\mathcal{F}\left(3\frac{h^2}{r^5} - \frac{1}{r^3}\right), \tag{A-3}$$

where $\mathcal{F}$ denotes the 2D Fourier transform.

The Fourier transform of $1/r^3$ is given by

$$I_1 = \int_{-\infty}^{\infty}\int_{-\infty}^{\infty}\frac{e^{-i(ux+vy)}}{[(x-\xi)^2 + (y-\eta)^2 + h^2]^{3/2}}\,\mathrm{d}x\mathrm{d}y = 4\int_0^{\infty}\int_0^{\infty}\frac{\cos ux\ \cos vy}{[(x-\xi)^2 + (y-\eta)^2 + h^2]^{3/2}}\,\mathrm{d}x\mathrm{d}y, \tag{A-4}$$

where u and v are the wavenumbers in the x- and y-directions, respectively. The integration over x can be carried out using expression 3.771.2 from Gradshteyn and Ryzhik (1980) to obtain

$$I_1 = 4u\int_0^{\infty}\cos vy\frac{1}{\sqrt{y^2+h^2}}K_1\left(u\sqrt{y^2+h^2}\right)\mathrm{d}y, \tag{A-5}$$

where K_1 is the modified Bessel function. The integration over y is carried out using expression 6.726.4 in Gradshteyn and Ryzhik (1980) to obtain

$$I_1 = \frac{2\pi}{h}e^{-h\sqrt{u^2+v^2}}, \tag{A-6}$$

The Fourier transform of $1/r^5$ is given by

$$I_2 = \int_{-\infty}^{\infty}\int_{-\infty}^{\infty}\frac{e^{-i(ux+vy)}}{[(x-\xi)^2 + (y-\eta)^2 + h^2]^{5/2}}\,\mathrm{d}x\mathrm{d}y = 4\int_0^{\infty}\int_0^{\infty}\frac{\cos ux\ \cos vy}{[(x-\xi)^2 + (y-\eta)^2 + h^2]^{5/2}}\,\mathrm{d}x\mathrm{d}y. \tag{A-7}$$

The first integration over u can be carried out using expression 3.771.2 in Gradshteyn and Ryzhik (1980) to obtain

$$I_2 = \frac{4}{3}u^2\int_0^{\infty}\cos vy\frac{1}{y^2+h^2}K_2(p\sqrt{y^2+h^2})dy. \tag{A-8}$$

The integration over y can now be carried out using expression 6.726.4 in Gradshteyn and Ryzhik (1980) to obtain

$$I_2 = \frac{2\pi}{3h^2}(\sqrt{u^2+v^2} + \frac{1}{h})e^{-h\sqrt{u^2+v^2}}. \tag{A-9}$$

By using equations A-6 and A-9, we obtain

$$\mathcal{F}\left(3\frac{h^2}{r^5} - \frac{1}{r^3}\right) = 3h^2 I_2 - I_1 = 2\pi\sqrt{u^2+v^2}e^{-h\sqrt{u^2+v^2}}, \tag{A-10}$$

and finally,

$$\mathcal{F}(B_z) = \frac{\mu_0}{2}\mathcal{F}(m)\sqrt{u^2+v^2}e^{-h\sqrt{u^2+v^2}}. \quad \text{(A-11)}$$

Taking into account that in the source-free region,

$$B_z = -\mu_0\frac{\partial V}{\partial z}, \quad \text{(A-12)}$$

where V is the magnetic potential, which is the same as the pseudogravity anomaly (Baranov, 1957) and we can write

$$\mathcal{F}(V) = \frac{1}{2}\mathcal{F}(m)e^{-h\sqrt{u^2+v^2}} = \mathcal{F}(g_{\text{pseudo}}). \quad \text{(A-13)}$$

After taking the inverse Fourier transform, the above equation becomes

$$m(\xi,\eta,h) = 2g_{\text{pseudo}}(\xi,\eta,h), \quad \text{(A-14)}$$

where $g_{\text{pseudo}}(\xi,\eta,h)$ is the pseudogravity anomaly measured on the surface $z = 0$ and downward continued to the depth of the equivalent source. This relationship is similar to that presented by Pedersen (1991) between magnetization and pseudogravity, which is an extension of the relationship between the magnetic pseudogravity and a magnetized half-space first presented by Grant and West (1965).

Because for a positively magnetized target, the pseudogravity anomaly is all positive, equation A-14 implies that all magnetic moments are also positive. Therefore, an all-positive equivalent source exists provided that the equivalent source is parametrized so that the dipole moments are chosen to be aligned with the inducing field direction. Given that the magnetization in the equivalent susceptibility layer under the inducing field satisfies this condition, the equivalent susceptibility is also positive.

The magnetic anomaly due to a general causative body is a linear superposition of dipole fields. Therefore, the conclusion from the dipole field is directly applicable to the field due to the extended sources.

The existence of an all-positive equivalent source applies equally well to the case when data are collected over any arbitrary 3D surface. To prove this, one can use Dirichlet's theorem and the fact that, from the data on a 3D surface, one can calculate the RTP field over any horizontal plane situated above the surface. Using again Dirichlet's theorem, the all-positive equivalent layer for this case will yield the measured field on the 3D surface.

REFERENCES

Baranov, V., 1957, A new method for interpretation of aeromagnetic maps: Pseudo-gravimetric anomalies: Geophysics, **22**, 359–382, doi: 10.1190/1.1438369.

Blakely, R., 1996, Potential theory in gravity and magnetic applications: Cambridge University Press.

Cordell, L., 1992, A scattered equivalent-source method for interpolation and gridding of potential field data in three dimensions: Geophysics, **57**, 629–636, doi: 10.1190/1.1443275.

Dampney, C. N. G., 1969, The equivalent source technique: Geophysics, **34**, 39–53, doi: 10.1190/1.1439996.

Dannemiller, N., and Y. Li, 2006, A new method for determination of magnetization direction: Geophysics, **71**, no. 6, L69–L73, doi: 10.1190/1.2356116.

Daubechies, I., 1992, Ten lectures on wavelets: SIAM.

Davis, K., and Y. Li, 2011, Fast solution of geophysical inversion using adaptive mesh, space-filling curves, and wavelet compression: Geophysical Journal International, **185**, 157–166, doi: 10.1111/j.1365-246X.2011.04929.x.

Fedi, M., G. Florio, and A. Rapolla, 1994, A method to estimate the total magnetization direction from a distortion analysis of magnetic anomalies: Geophysical Prospecting, **42**, 261–274, doi: 10.1111/j.1365-2478.1994.tb00209.x.

Gerovska, D., M. J. Araúzo-Bravo, and P. Stavrev, 2009, Estimating the magnetization direction of sources from southeast Bulgaria through correlation between reduced-to-the-pole and total magnitude anomalies: Geophysical Prospecting, **57**, 491–505, doi: 10.1111/j.1365-2478.2008.00761.x.

Gradshteyn, I. S., and I. W. Ryzhik, 1980, Table of integrals, series, and products: Academic Press.

Grant, F. S., and G. F. West, 1965, Interpretation theory in applied geophysics: McGraw-Hill.

Hansen, R. O., and Y. Miyazaki, 1984, Continuation of potential fields between arbitrary surfaces: Geophysics, **49**, 787–795, doi: 10.1190/1.1441707.

Hansen, R. O., and R. S. Pawlowski, 1989, Reduction to the pole at low latitude by Wiener filtering: Geophysics, **54**, 1607–1613, doi: 10.1190/1.1442628.

Keating, P., and L. Zerbo, 1996, An improved technique for reduction to the pole at low latitudes: Geophysics, **61**, 131–137, doi: 10.1190/1.1443933.

Li, Y., and D. W. Oldenburg, 2001, Stable reduction to the pole at the magnetic equator: Geophysics, **66**, 571–578, doi: 10.1190/1.1444948.

Li, Y., and D. W. Oldenburg, 2003, Fast inversion of large-scale magnetic data using wavelet transforms and a logarithmic barrier method: Geophysics Journal International, **152**, 251–265.

Li, Y., and D. W. Oldenburg, 2010, Rapid construction of equivalent sources using wavelets: Geophysics, **75**, no. 3, L51–L59, doi: 10.1190/1.3378764.

Mendonca, C. A., and J. B. C. Silva, 1993, A stable truncated series approximation of the reduction-to-the-pole operator: Geophysics, **58**, 1084–1090, doi: 10.1190/1.1443492.

Nocedal, J., and S. J. Wright, 1999, Numerical optimization: Springer Science.

Parker, R. L., 1994, Geophysical inverse theory: Princeton University Press.

Pawlowski, R. S., 1994, Green's equivalent-layer concept in band-pass filter design: Geophysics, **59**, 69–76, doi: 10.1190/1.1443535.

Pearson, W. C., and C. M. Skinner, 1982, Reduction-to-the-pole of low latitude magnetic anomalies: Presented at the 52nd Annual International Meeting, SEG, Expanded Abstracts, 356–358.

Pedersen, L. B., 1991, Relations between potential fields and some equivalent sources: Geophysics, **56**, 961–971, doi: 10.1190/1.1443129.

Phillips, J., 2005, Can we estimate total magnetization directions from aeromagnetic data using Helbig's formulas: Earth, Planets and Space, **57**, 681–689, doi: 10.1186/BF03351848.

Silva, J. B. C., 1986, Reduction-to-the-pole as an inverse problem and its application to low-latitude anomalies: Geophysics, **51**, 369–382, doi: 10.1190/1.1442096.

Wright, S. J., 1997, Primal-dual interior-point methods: SIAM.